

GAMMA-RAY OBSERVATIONS OF NGC 253 AND M82 WITH OSSE

D. BHATTACHARYA,¹ L.-S. THE,² J. D. KURFESS,³ D. D. CLAYTON,² N. GEHRELS,⁴
 M. D. LEISING,² D. A. GRABELSKY,⁵ W. N. JOHNSON,³ G. V. JUNG,⁶
 R. L. KINZER,³ W. R. PURCELL,⁵ M. S. STRICKMAN,³ AND
 M. P. ULMER⁵

Received 1993 December 14; accepted 1994 June 15

ABSTRACT

Gamma-ray observations of the nearby starburst galaxies NGC 253 and M82 over the energy range (0.05–10) MeV have been obtained with the OSSE spectrometer on the *Compton Gamma-Ray Observatory*. The priority of these galaxies as OSSE targets had been established on the grounds that the average supernova rate may be high in starbursts as indicated by infrared and radio observations, and at distances of ~ 3 Mpc a significant chance of supernova γ -ray line detection exists. NGC 253 was detected in continuum emission up to 165 keV with a total significance of 4.4σ and an estimated luminosity of 3×10^{40} ergs s^{-1} . The spectrum is best fit by a power law of photon index ~ 2.5 . We consider the possible contribution of different emission mechanisms, including inverse Compton scattering, bremsstrahlung, discrete sources, and Type Ia/Ib supernova continuum to the measured flux. No significant continuum flux was observed from M82. A search for the γ -ray line from the decay of the most abundant radioactive element produced in supernovae ($^{56}\text{Ni} \rightarrow ^{56}\text{Co} \rightarrow ^{56}\text{Fe}$) yielded no significant detection: the 3σ upper limits to the line fluxes at 0.158, 0.812, 0.847, and 1.238 MeV for both galaxies are obtained.

Subject headings: galaxies: starburst — galaxies: individual (NGC 253, M82) — gamma rays: observations — radiation mechanisms: nonthermal

1. INTRODUCTION

NGC 253 and M82 (NGC 3034), two of the brightest infrared galaxies, are considered prototypical starburst galaxies. Although both galaxies exhibit extensive star formation activity in their cores, they differ in their morphologies and in their associations with other nearby galaxies. It is suggested that the gravitational interaction with the giant spiral galaxy M81 has caused matter to fall into the nuclear region of M82 and initiate accelerated star formation through shock waves (Kronberg, Biermann, & Schwab 1985). The high star formation phenomenon also implies a high supernova rate. The powerful outflowing wind generated by such supernova activity may have given rise to nuclear outflows (e.g., model of Clegg & Chevalier 1985) as evidenced in the detection of an extended X-ray emission (Watson, Stanger, & Griffiths 1984; Schaaf et al. 1989), nonthermal radio halo (Seaquist & Odegard 1991), and optical emission lines (McCarthy, Heckman, & van Breugel 1987; Bland & Tully 1988) from the surroundings of M82. Similar nuclear outflows have been observed in NGC 253 where the *Einstein* IPC images have revealed a plume of X-ray emission extending above the galactic plane (Fabbiano & Trinchieri 1984). Within the inner core (~ 600 pc) of NGC 253 at least 35 compact radio sources have been discovered (Antonucci & Ulvestad 1988) and the *Einstein* HRI imager has identified eight discrete X-ray sources in the central 500 pc (Fabbiano & Trinchieri 1984).

It is not clear what particular mechanism gives rise to the starburst event. The progenitor of such a phenomenon could be the efficient use of the abundant interstellar medium in the starburst core (e.g., in NGC 253) or an extensive supply of gas from the surrounding intergalactic medium (e.g., in M82). The starburst models of Rieke et al. (1980), in order to simultaneously match the luminosity, color, and dynamical mass of the galaxy, are biased toward producing massive stars. These stars, being luminous and massive ($3\text{--}100 M_{\odot}$), have very short lifespans with most of them resulting in supernovae. It is believed that the massive C/O Wolf-Rayet stars undergo strong mass loss and explode as Type Ib SNs, whereas O and B stars generally evolve into Type II SNs (Melnick & Terlevich 1988). Initial estimates of supernova rates obtained from radio observations of M82 and NGC 253 (Bartel et al. 1987; Antonucci & Ulvestad 1988) are in the range (0.1–0.3) supernova per yr within the inner 600 pc for those galaxies, but recent observations of Ulvestad & Antonucci (1994) suggest that the rate could be considerably lower.

Clayton, Colgate, & Fishman (1969) predicted that core collapse supernova would give rise to γ -ray lines due to the decay of ^{56}Ni , which is produced abundantly during the explosion. The detection of ^{56}Co (e.g., Leising & Share 1990, and references therein) and ^{57}Co (Kurfess et al. 1992) γ -ray lines from SN 1987A has confirmed this prediction and γ -ray observations have emerged as a promising diagnostic tool of supernova nucleosynthesis. Gamma-ray observations of starburst galaxies which are indicated by radio and infrared observations to have a high supernova rate, may serve a promising role with its potential to detect supernovae signatures through the dense starburst nuclear regions. Such observations could be used as a direct estimator of supernova rates and discern between different types of supernovae occurring in the starburst cores. The γ -ray line and continuum fluxes of massive star supernovae have been calculated by many investigators

¹ Institute of Geophysics and Planetary Physics, University of California, Riverside, CA 92521.

² Department of Physics and Astronomy, Clemson University, Clemson, SC 29634-1911.

³ E. O. Hulbert Center for Space Research, Naval Research Laboratory, Mail Code 76540, Washington, DC 20375-5352.

⁴ Code 661, NASA/Goddard Space Flight Center, Greenbelt, MD 20771.

⁵ Department of Physics and Astronomy, Northwestern University, Evanston, IL 60208.

⁶ Universities Space Research Association, Washington, DC 20024.

(Pinto & Woosley 1988; Woosley, Pinto, & Hartmann 1989; Nomoto et al. 1988; Bussard, Burrows, & The 1989; The, Burrows, & Bussard 1990; Chan & Lingenfelter 1991). Ensmann & Woosley (1988) have constructed detailed evolutionary models of Wolf-Rayet stars and find that only 4–6 M_{\odot} models produce the best fit to light curves of Type Ib supernovae. The γ -ray lines from these models peak between 3.1×10^{-5} to $4.4 \times 10^{-4} \gamma \text{ cm}^{-2} \text{ s}^{-1}$ at a distance of 1 Mpc. Nomoto, Kumagai, & Shigeyama (1991), in their calculations of He star explosions, find the range of γ -ray line fluxes to be 3.9×10^{-5} to $8.8 \times 10^{-4} \gamma \text{ cm}^{-2} \text{ s}^{-1}$ at a distance of 1 Mpc. This indicates that OSSE has a potential range out to 4 Mpc for detecting ($\sim 3 \sigma$) Type Ib supernovae.

It is generally believed that only old binary systems produce Type Ia supernovae, so their rates are unlikely to be enhanced in starburst cores. Although a number of theoretical models for Type Ia supernovae have been formulated, the progenitors of such explosions could still come from a wide range of stellar populations. Hence, we do not preclude the possibility of Type Ia events in starburst nuclei. The ^{56}Co 0.847 MeV γ -ray line arising from a Type Ia SN at 1 Mpc distance could produce a peak flux of $3.5 \times 10^{-3} \gamma \text{ cm}^{-2} \text{ s}^{-1}$ (Burrows & The 1990). With a two week observation period this line can be detected by OSSE at a 3σ significance level up to a distance of 10 Mpc.

NGC 253 and M82 are relatively nearby galaxies, located at estimated distances of ~ 3.4 Mpc and 3.25 Mpc, respectively. For our calculations, we have used an approximate number of 3.3 Mpc for both these galaxies. A Type Ia or Ib SN explosion in these galaxies has the potential of getting detected at $\geq 3 \sigma$ level. The reasonable probability of detecting SN line and continuum fluxes make M82 and NGC 253 priority targets for γ -ray observing instruments. In this paper, we present the results of the first low-energy γ -ray observation of these two galaxies by the *Compton Gamma-Ray Observatory's* (CGRO) Oriented Scintillation Spectrometer Experiment (OSSE).

2. OBSERVATIONS AND RESULTS

The OSSE instrument, which is sensitive to γ -rays in the range 0.05–10 MeV, is designed to study the nucleosynthesis from cosmic sources by detecting γ -ray lines from radioactive elements. The OSSE instrument consists of four actively shielded NaI(Tl)–CsI(Na) phoswich detectors. Each of the detectors has a $3^{\circ}8 \times 11^{\circ}4$ (FWHM) field of view. A detailed description of the instrument also describing the characteristics and performance can be found in Johnson et al. (1993).

The background fields for the observations were obtained by moving the detectors by 4.5 degrees to either side of the source position on the scan plane. The accumulation schedule for each of the four detectors alternated about every 130 seconds between source observations and background measurements. A quadratic background estimation is performed by fitting three or four background observations accumulated before

and after the source observation (Johnson et al. 1993). Background subtraction for each detector is carried out and the individual difference spectra for each detector are summed and stored in a spectrum database (SDB) file along with other housekeeping and environmental parameters. Several environmental data selection criteria such as rigidity, time from the last SAA passage, and anticoincident shield rates to remove systematics effects arising from spacecraft orbital variations are imposed. Spectral deconvolution is performed by folding a model photon spectrum through instrument response matrices. The resulting count spectrum is compared with the data and the model parameters are modified to achieve the best fit.

2.1. NGC 253

NGC 253 is located very near to the Galactic south pole. The galaxy was observed with OSSE in six separate viewing periods, during the Phase 1 (1st year) and Phase 2 (2d year) cycle of the *Compton Gamma-Ray Observatory*, for a total observation time of $\sim 10^6$ s. Two of these observations were carried out with a different scan mode and consequently had little source exposure; these viewing periods were not analyzed. The observation schedule of the relevant viewing periods are shown in Table 1, column (1) denotes the *Compton* viewing period number, column (2) shows the dates of observation, column (3) gives exposure times in seconds and column (4) the total number of detectors used in the observation.

The four viewing periods (VP) of Table 1 are combined and analyzed as one data set (Set I). This set represents the total (Phase 1 + Phase 2) data. A second data set (Set II) comprising only the first three VPs (or Phase 1) is analyzed separately. We have used simple power law models to obtain the continuum photon fluxes. The emission spectrum of Set I is best fit by a power law with a photon index of 2.55 ± 0.45 ($\chi^2 = 12.01$, ndof = 11). The index of Set II is 2.78 ± 0.79 ($\chi^2 = 12.28$, ndof = 11). In Table 2 the measured fluxes for Set I are shown. The significance of this detection is 4.4σ . The flux over the 50–165 keV band is $3 \times 10^{-11} \text{ ergs cm}^{-2} \text{ s}^{-1}$ with an estimated luminosity of $3 \times 10^{40} \text{ ergs s}^{-1}$.

The derived photon spectrum obtained from the data set I is shown in Figure 1. At X-ray energies, fluxes measured by *Ginga* over the energy range 2–10 keV, and by *HEAO A4* in 20–150 keV (Gruber & MacDonald 1993) are also given. The *Ginga* photon fluxes were estimated from the spectral fitting parameters given by Ohashi et al. (1990) who find that both thermal bremsstrahlung and power law models give acceptable fits to *Ginga* results, although they prefer a thermal spectrum with $kT \sim 6$ keV because the derived N_{H} for the power-law model is much higher than the Galactic value and contradicts the *Einstein* IPC results. We estimate the *Ginga* photon fluxes from their power-law spectral parameters (with a photon index of 2.31, +0.14, –0.19) and show that even a power-law extrapo-

TABLE 1
NGC 253 OBSERVATIONS BY OSSE

Viewing Period (1)	Date (2)	Exposure (s) (3)	Number of Detectors (4)
9	1991 Sep 5 16:13–1991 Sep 11 23:34	3.54×10^5	4
13.5	1991 Nov 7 18:20–1991 Nov 14 17:06	1.34×10^5	4
16	1991 Dec 14 01:40–1991 Dec 28 18:06	3.08×10^5	2
211	1993 Feb 25 17:20–1993 Mar 9 13:36	1.40×10^5	2

TABLE 2
RESULTS OF FOUR NGC 253 OBSERVATIONS BY OSSE

Energy Bins (MeV)	Flux (photons $\text{cm}^{-2} \text{s}^{-1} \text{MeV}^{-1}$)
0.05 – 0.06	$(4.83 \pm 3.36) \times 10^{-3}$
0.06 – 0.07	$(4.15 \pm 2.60) \times 10^{-3}$
0.07 – 0.09	$(1.43 \pm 1.17) \times 10^{-3}$
0.09 – 0.11	$(1.38 \pm 0.61) \times 10^{-3}$
0.110– 0.135	$(8.70 \pm 4.73) \times 10^{-4}$
0.135– 0.165	$(11.14 \pm 5.16) \times 10^{-4}$
0.165– 0.200	$(-1.60 \pm 6.12) \times 10^{-4}$
0.200– 0.300	$(2.92 \pm 2.73) \times 10^{-4}$
0.300– 0.500	$(0.43 \pm 1.75) \times 10^{-4}$
0.500– 1.000	$(0.15 \pm 1.40) \times 10^{-4}$
1.000– 3.000	$(0.87 \pm 4.61) \times 10^{-5}$
3.000– 5.000	$(-0.31 \pm 1.78) \times 10^{-5}$
5.000–10.000	$(4.58 \pm 5.02) \times 10^{-6}$

lation of *Ginga* data into the OSSE regime yields fluxes an order of magnitude below the OSSE data points. We have searched the *Einstein* IPC and HRI database to look for a possible counterpart of the measured emission. We found four 1E sources residing within 2 degrees of the galaxy but outside its core. Each of the sources has an average flux value of less than $10^{-12} \text{ ergs cm}^{-2} \text{ s}^{-1}$. We assume that these sources are not the origin of the measured emission. A search of the NASA/IPAC Extragalactic Data base failed to show any X-ray bright objects within a circle of radius 2° around NGC 253. The discussion on the possible origins of the OSSE flux is deferred until § 3.

An interesting feature of γ -ray observations of a starburst galaxy with its high supernova rate discussed in the introduction is the possibility of detecting γ -line supernova. A line search was carried out at energies corresponding to lines from $^{56}\text{Ni} \rightarrow ^{56}\text{Co}$ decay at 0.158 and 0.812 MeV and from $^{56}\text{Co} \rightarrow ^{56}\text{Fe}$ decay at 0.847 and 1.238 MeV. The ^{56}Ni is the most abundant radioactive isotope produced during a supernova event and provides the power for the supernova light curves at late times when the light curve decreases exponentially. In order to determine possible line fluxes a Gaussian fit at the line center energies were performed. The line widths were fixed and the corresponding center energies were also fixed. One sigma errors were calculated by finding the deviation of the line flux necessary to increase the minimum value of chi-square by 1 (single parameter determination). The line widths are taken as 3.5% of the rest energy following the calculation of Chan & Lingenfelter (1991) for a Type Ia supernova. The search failed to show any significant flux. The 3σ upper limits to the fluxes for 0.158, 0.812, 0.847, and 1.238 MeV lines are given in Table 4 below. The upper limits are calculated for each individual VP and also for data Set I.

TABLE 3
M82 OBSERVATIONS BY OSSE

Viewing Period	Date	Exposure (s)	Number of Detectors
7	1991 Aug 9 04:11–1991 Aug 15 18:28	3.22×10^5	4
18	1992 Jan 10 17:31–1992 Jan 23 19:41	7.20×10^5	4
216	1993 Apr 6 14:22–1993 Apr 12 15:24	3.31×10^5	4
218	1993 Apr 20 00:00–1993 May 4 01:01	5.76×10^5	4
227–228	1993 Jun 29 14:22–1993 Jul 27 14:27	1.83×10^6	4

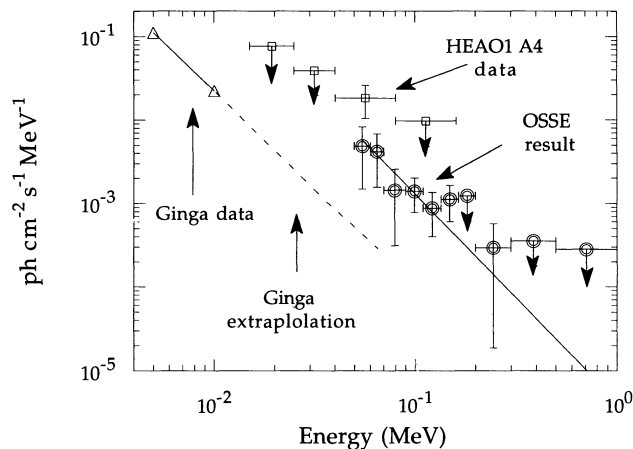


FIG. 1.—Derived photon fluxes for NGC 253. The *Ginga* X-ray points and their extrapolation to higher energies are also shown. HEAO A4 data and upper limits are also displayed for comparison.

2.2. M82

OSSE observed M82 during viewing periods 7 (1991 August 9–15) and 18 (1992 January 10–23). The large field of view of OSSE also observed M82 during observations of SN 1993J in M81 in viewing periods 216 (1993 April 6–12), 218 (1993 April 20–May 4), and 227–228 (1993 June 29–July 27). The observation schedule is given in Table 3. We fit the count spectrum to a Gaussian γ -ray line feature centered at energy 0.158, 0.812, 0.847, or 1.238 MeV with 3.5% rest energy line widths. We find no evidence for ^{56}Ni and ^{56}Co line emissions. The results of that fit are presented as 3σ upper limits in Table 4 for the best-fit γ -line fluxes at 0.158, 0.812, 0.847, and 1.238 MeV.

We see no evidence for continuum emission from M82 during viewing periods 7 and 18. The 3σ upper limit to the (50–200) keV continuum flux is $4.3 \times 10^{-3} \text{ photons cm}^{-2} \text{ s}^{-1} \text{ MeV}^{-1}$. In Figure 2 we present the upper limits to the continuum fluxes of M82. Leising et al. (1994) detected excess continuum fluxes below 200 keV during OSSE SN 1993J observations (viewing periods 216, 218, and 227–228), the origin of which was probably due to the interaction of the fast supernova ejecta with circumstellar material surrounding SN 1993J in M81. The 50–200 keV continuum fluxes from M81/M82 during viewing period 216 was detected at 4.5σ level (Leising et al. 1994). Therefore, these viewing periods are excluded from the M82 continuum flux analysis. The HEAO A4 fluxes (Gruber & MacDonald 1993) and EXOSAT X-ray measurements (Schaaf et al. 1989) are also shown in Figure 2. HEAO A4 points can be adequately described as a power-law extrapolation of the EXOSAT data points (which can be fitted both by a power law of index ~ 1.75 and thermal emission from hot gas with $kT \sim 9 \text{ keV}$). We find the upper limits of

TABLE 4
3 SIGMA UPPER LIMITS TO THE LINE FLUXES FROM NGC 253 AND M82

Galaxy	VP	158 keV	812 keV	847 keV	1238 keV
NGC 253	9	7.9×10^{-5}	1.9×10^{-4}	1.8×10^{-4}	1.9×10^{-4}
	13.5	1.1×10^{-4}	2.9×10^{-4}	2.0×10^{-4}	2.6×10^{-4}
	16	1.1×10^{-4}	1.6×10^{-4}	1.3×10^{-4}	1.9×10^{-4}
	211	1.4×10^{-4}	2.1×10^{-4}	2.0×10^{-4}	3.6×10^{-4}
	Phase 1 + 2	6.7×10^{-5}	1.0×10^{-4}	1.0×10^{-4}	1.2×10^{-4}
M82	7	8.6×10^{-5}	1.7×10^{-4}	2.2×10^{-4}	2.3×10^{-4}
	18	5.2×10^{-5}	1.3×10^{-4}	1.5×10^{-4}	1.0×10^{-4}
	7 + 18	4.2×10^{-5}	1.0×10^{-4}	1.3×10^{-4}	9.7×10^{-5}
	216	1.2×10^{-4}	1.8×10^{-4}	1.4×10^{-4}	2.3×10^{-4}
	218	1.3×10^{-4}	1.4×10^{-4}	1.3×10^{-4}	1.8×10^{-4}
	227–228	5.0×10^{-5}	7.4×10^{-5}	7.7×10^{-5}	9.8×10^{-5}

OSSE M82 photon continuum of viewing periods 7 and 18 below 100 keV are consistent with *HEAO* A4 measurements below 80 keV. However, the *HEAO* A4 observed data point near 100 keV for M82 is above the 2σ upper limits of OSSE M82 continuum near 100 keV.

3. DISCUSSION

Rephaeli et al. (1991) deduced a mean X-ray spectrum for a sample of 53 *IRAS*-selected candidate starburst galaxies using the *HEAO* 1 A2 and A4 data base. Their mean starburst galaxy spectrum, over the energy range 0.5–80 keV, has a power-law index of 1.0 ± 0.3 , flatter than the mean AGN spectrum, with a power-law index of 1.62 ± 0.04 as estimated by Rothschild et al. (1983). The integrated mean X-ray flux over the energy range 0.06–0.2 MeV agrees within a factor of 2 with the continuum emission measured from NGC 253. The origin of hard X-rays or low-energy γ -rays in a starburst galaxy would include inverse Compton effects, electron bremsstrahlung or thermal emission from hot supernova ejecta. Discrete sources such as X-ray binaries or individual supernova outbursts may also contribute substantially to the emission.

3.1. Diffuse Emission

The contribution of inverse Compton scattering of relativistic electrons off the far infrared (FIR) photon field to the

total X-ray emission in starburst galaxies has been considered before with respect to M82 (Schaaf et al. 1989; Seaquist & Odegard 1991). The emission in the radio range is assumed to be primarily of synchrotron origin and coming from the same set of relativistic electrons responsible for the inverse Compton emission. For NGC 253 the FIR photon energy density is calculated from the total FIR luminosity given by Soifer et al. (1987). *IRAS* Small Structure Catalog (1988) gives the spatial extent of the 100 μm source to be 2.5 which at a distance of ~ 3 Mpc corresponds to ~ 2 kpc. The thickness of the disk is assumed to be 300 pc. Hence, an emitting volume, V , of $2.5 \times 10^{64} \text{ cm}^3$ has been used for the calculation. Using the radio spectral data given by Klein et al. (1983) our estimated IC luminosities for NGC 253, in the range 0.05–0.165 MeV, for magnetic field values of 1 and 5 μG , are 6×10^{39} and $4 \times 10^{38} \text{ ergs s}^{-1}$, respectively. The observed luminosity over the same energy range is $\sim 3 \times 10^{40} \text{ ergs s}^{-1}$. Even given the uncertainties in such calculations we find that inverse Compton scattering accounts for only a small fraction of the emission seen in NGC 253. Similar calculation for M82 yield an inverse Compton luminosity in energy range 50–200 keV of $\sim 5 \times 10^{39} \text{ ergs s}^{-1}$ which is consistent with upper limits we obtain from OSSE observations of M82.

At 100 keV, the bremsstrahlung contribution could be at least a factor of 2 higher than inverse Compton scattering in our Galaxy. Hence, it is not unlikely that the bremsstrahlung contribution could be large in the NGC 253, but a proper estimation would require a better understanding of the cosmic ray and nucleon density in NGC 253 core. Using the bremsstrahlung emissivity given by Skibo & Ramaty (1992) and considering an emitting volume, V , as given above, we derive the following expression for bremsstrahlung luminosity:

$$L_{\text{brem}} = 4 \times 10^{34} \rho_{\text{cr}} \rho_{\text{ism}} \text{ ergs s}^{-1} \quad (1)$$

for a local interstellar density, N_{H} of 0.25 cm^{-3} . Here, ρ_{cr} is the ratio of the equilibrium electron spectra of NGC 253 to that of the local equilibrium electron spectra and ρ_{ism} is the ratio of the interstellar density of NGC 253 to that of the local interstellar density. We adopt the value of ρ_{cr} to be ~ 160 as given by Völk, Klein, & Wielebinski (1989) for M82, although such estimation is highly uncertain. Assuming that this ratio also holds for NGC 253 and taking its interstellar density, N_{H} , to be $\sim 30 \text{ cm}^{-3}$ (Rieke et al. 1980), we find the total bremsstrahlung luminosity to be $\sim 10^{39} \text{ ergs s}^{-1}$. This value is approximately 3% of the observed luminosity.

Hence, the combined contribution of the bremsstrahlung and inverse Compton effect to the low-energy γ -ray regime

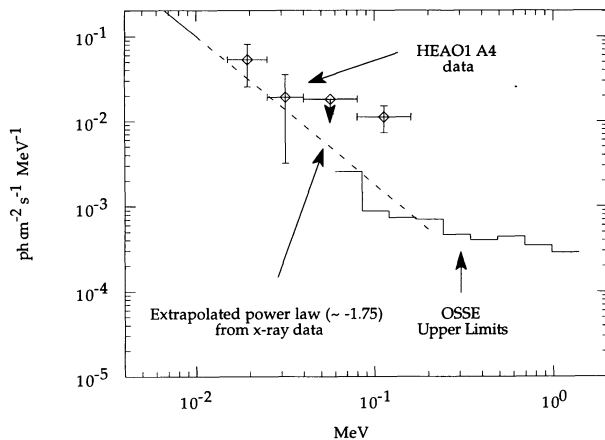


FIG. 2.—Derived X- and γ -ray photon fluxes and continuum upper limits for M82. The data points with diamond characters are the *HEAO* A4 measurements. The dashed line is an extrapolation of the power-law fit with index of ~ -1.75 to *EXOSAT* X-ray data. The upper limits of OSSE M82 measurement are the 2σ upper limits.

may provide only a fraction of the observed NGC 253 flux, unless ρ_{cr} is really large ($\sim 10^3$) in starbursts. In the X-ray range, inverse Compton effect may provide a considerable part ($\sim 50\%$) of the entire X-ray luminosity, although Ohashi et al. (1990) consider that 20%–60% of the X-ray emission in (2–20) keV may come from isothermal hot gas created during repeated supernova explosions.

3.2. Discrete Sources

Fabbiano & Trinchieri (1985) estimate the contribution from discrete sources in 0.2–4.0 keV to be around 4.4×10^{39} ergs s^{-1} which is approximately 40% of the observed X-ray luminosity. Ohashi et al. (1990) argue that LMXBs are not a part of these discrete sources as the typical lifetime of LMXBs are significantly longer ($\geq 10^9$ yr) than the estimated starburst time ($\sim 10^7$ yr). The emission from young, massive Population I binary X-ray sources (with $kT \geq 10$ keV) can be a component of the hard X-ray spectrum, but the number of such sources needed to explain the OSSE NGC 253 flux would be in the range of 10^3 – 10^4 . Although such a number is not totally unreasonable for starburst galaxies, there is no evidence that their spectra extend above 100 keV.

The infrared and X-ray luminosities of M82 are comparable to those of NGC 253. If the measured flux from NGC 253 originates mostly from diffuse mechanisms then one would expect similar fluxes from M82 which is located almost at the same distance as NGC 253. If the discrete source contribution is dominant in NGC 253, then the absence of any significant observable flux from M82 may imply the existence of different environments within starburst galaxies. The *HEAO* A4 detection of M82 up to 40 keV (see Fig. 2) may indicate a non-thermal component in addition to the thermal spectrum observed by *Ginga* and *EXOSAT*. Further observation of M82 is necessary to ascertain the existence or variability of this nonthermal component.

3.3. Supernova Continuum

We also consider the possibility that part of the detected continuum emission from NGC 253 can arise from a Type Ia or Ib SN outburst in NGC 253 but with γ -ray lines obscured by overlying ejecta material (e.g., at the early times of SN explosion). The continuum emission is due to photons in the γ -ray lines of the radioactive decay chain of ^{56}Ni which are degraded in energy through Compton down-scattering in the expanding envelope. Expected γ -ray spectra for a Type Ia and a Type Ib supernova near their peak hard X-ray luminosity scaled to the distance of NGC 253 are shown in Figure 3. We compare this with NGC 253 flux evaluated only from VPs 9, 13.5, and 16. We find that the γ -ray transport calculations of Burrows & The (1990) for a Type Ia SN (model WW2 of Woosley & Weaver 1986), when scaled to the distance of NGC 253, predict continuum flux values at 100 keV (at day 20–100) at the same level as the detected flux from NGC 253. However, the peak 847 keV flux for a Type Ia SN (WW2 model) occurs at day ~ 70 and is $3 \times 10^{-4} \gamma \text{ cm}^{-2} \text{ s}^{-1}$. The absence of this line in the observations makes it unlikely that the continuum emission is due to a Type Ia SN. We consider Type Ia SN here because some models predict that, in star-forming regions, the evolution of massive stars ($\geq 8 M_{\odot}$) in close binaries might terminate as Type Ia SNs within a short timescale (\sim few times 10^7 years; Iben & Tutukov 1984). Similar calculations of γ -ray fluxes (Model WR6C of The, Clayton, & Burrows 1991) carried

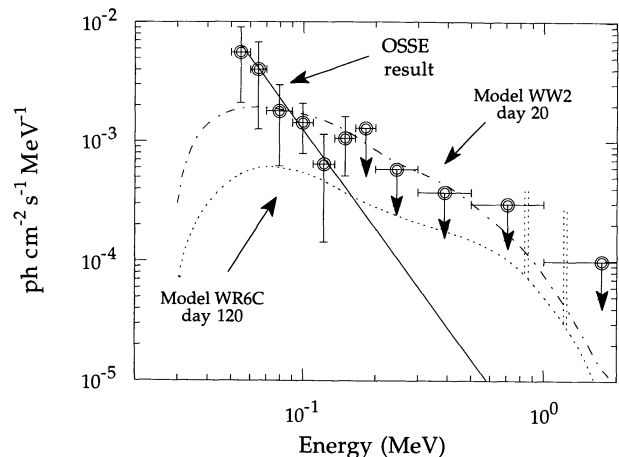


FIG. 3.—Continuum emissions from a Type Ia (Model WW2) and a type Ib SN (Model WR6C) are compared with the observed flux from NGC 253. The NGC 253 fluxes are obtained from VPs 9, 13.5, and 16. The 0.847 and 1.238 MeV lines of WW2 are not shown for clarity.

out from a Type Ib Wolf-Rayet SN (Ensmann & Woosley 1988) yield peak continuum flux values (at day 80–150) at factors of 4–5 lower than what have been observed. Given the uncertainties involved in the estimation of the diffuse emission, discrete source contribution, parameters of the SN model and distance to NGC 253, it remains a possibility that a Type Ib explosion could contribute to the observed continuum fluxes. Furthermore, the peak flux in the 847 keV line for WR6C model ranges from 3.4×10^{-6} to $5 \times 10^{-5} \gamma \text{ cm}^{-2} \text{ s}^{-1}$ and would not have been detected by OSSE. The difference between the OSSE measurements and the extrapolation of the *Ginga* data may also be understood in terms of a short-term hard X-ray supernova continuum. The models WW2 and WR6C are used only for illustration purposes; the detailed structure of the spectrum depends on the ejecta mass, expansion velocity and Compton opacities of the supernova.

3.4. Supernova Rates

Monte Carlo simulations of randomly occurring supernova events in NGC 253 and M82 were performed to evaluate the significance of our upper limit to the 0.847 and 1.238 MeV ^{56}Co γ -ray line fluxes on the supernova rate from these two galaxies. For this purpose we take the 3σ upper limit to be the best-fit value plus three standard deviations from that value. The 3σ upper limits to the 0.847 MeV γ -line fluxes from two VPs of M82 plus three VPs of SN 1993J observations which occurred in M81, the companion galaxy of M82 and four VPs of NGC 253 were compared with the line fluxes generated by the Monte Carlo histories. The 3σ upper limits to the 847 line fluxes during these nine VPs are given in Table 4. We assume that supernova rates are the same in all starbursts. Based on the nondetection of γ -ray lines during the observations of M82 and NGC 253 and Monte Carlo simulations, we derive the 3σ upper limits to the supernova rates to be 1.9, 1.6, 6.3, and 3.0 yr^{-1} for models W7, W7 with total γ -line escape ($f_{\text{escp}} = 1$), WR 6C and WR 6Cfm with $f_{\text{escp}} = 1$, respectively. Model W7 is a Type Ia supernova deflagration model of a carbon-oxygen white dwarf thermonuclear explosion (Nomoto et al. 1984). WR 6C is a Type Ib supernova model of Wolf-Rayet progenitor (Ensmann & Woosley 1988).

Although our initial upper limits for supernova rate estimates are not as restrictive as the radio limits, we should mention that gamma-ray observations provide a direct estimation of Type Ia SN rates (to date no Type Ia SN has been observed in the radio wavelengths). A combination of the gamma-ray and radio limits can provide useful limits.

In view of the cosmic ray rich environment of the starburst galaxies, one would expect high-energy γ -rays due to increased rate of nucleon-nucleon collision. Estimations of such process (Völk et al. 1989; Akyüz, Brouillet, & Özel 1991) predict, at best, marginal detection of M82 by the EGRET instrument above 300 MeV. Recent EGRET results of NGC 253 and M82 have only provided upper limits (Sreekumar et al. 1994). Hence, it seems low-energy γ -ray observations offer us the best possibility to obtain direct estimation of supernova rates in starburst cores and cosmic-ray yields through continuum and line observations.

4. SUMMARY

Low energy γ -ray observations of NGC 253 and M82 by the OSSE instrument on-board *Compton Gamma-Ray Observatory* are presented. NGC 253 was detected up to 165 keV with a total significance of 4.4σ and an estimated luminosity of 3×10^{40} ergs s^{-1} . For the measured continuum we suggest the

observed emission can be a combination of inverse Compton, bremsstrahlung and discrete source emission. We also show the possibility of a Type Ib SN continuum emission contributing to the observed flux. The 3σ upper limits for 0.158, 0.812, 0.847, and 1.238 MeV line fluxes are presented. The two viewing periods 7 and 18 of M82 observations by OSSE only obtained upper limits of γ -ray continuum fluxes. The 3σ upper limits for γ -ray line fluxes from M82 are also presented.

Comparing the γ -ray line upper limits with Monte Carlo simulations, we find that for Type Ia and for some Type Ib supernova models the 3σ upper limits to the rates are 1.9 and 6.3 yr^{-1} , respectively. Although the constraint from γ -ray line nondetection only confirmed the previous limits to the supernova rates in these galaxies obtained by infrared and radio observations, frequent *CGRO* observations combined with the radio measurements can put stronger limits on these rates.

It is a pleasure to acknowledge the assistance of Byron Leas, Kelly McNaron-Brown, and Chris Starr for providing supporting analysis tools. We thank Charles Dermer and Jeff Skibo for useful discussion. D. B. wishes to thank the members of IGPP, UC Riverside for providing valuable assistance. This work was supported under NASA grant DPR S-10987C and an OSSE Phase 1 Guest Investigation Program.

REFERENCES

- Akyüz, A., Brouillet, N., & Özel, M. E. 1991, *A&A*, 248, 419
 Antonucci, R. R. J., & Ulvestad, J. S. 1988, *ApJ*, 330, L97
 Bartel, N., et al. 1987, *ApJ*, 323, 505
 Bland, I., & Tully, R. B. 1988, *Nature*, 334, 43
 Burrows, A., & The, L.-S. 1990, *ApJ*, 360, 626
 Bussard, R. W., Burrows, A., & The, L.-S. 1989, *ApJ*, 346, 395
 Chan, K. W., & Lingenfelter, R. E. 1991, *ApJ*, 368, 515
 Clegg, A. W., & Chevalier, R. A. 1985, *BAAS*, 17, 587
 Clayton, D. D., Colgate, S. A., & Fishman, G. 1969, *ApJ*, 155, 75
 Ensmann, L., & Woosley, S. E. 1988, *ApJ*, 333, 754
 Fabbiano, G., & Trinchieri, G. 1984, *ApJ*, 286, 491
 ———. 1985, *ApJ*, 296, 430
 Gruber, D., & MacDonald, D. 1993, private communication
 Iben, I., & Tutukov, A. 1984, *ApJ*, 54, 335
IRAS Small Scale Structure Catalog. 1988, prepared by G. Helou & D. W. Walker (Washington: GPO)
 Johnson, W. N., et al. 1993, *ApJS*, 86, 693
 Klein, U., Urbanik, M., Beck, R., & Wiełbinski, R. 1983, *A&A*, 127, 177
 Kronberg, P. P., Biermann, P., & Schwab, F. R. 1985, *ApJ*, 291, 693
 Kurfess, J. D., et al. 1992, *ApJ*, 399, L137
 Leising, M. D., & Share, G. H. 1990, *ApJ*, 357, 638
 Leising, M. D., et al. 1994, *ApJ*, 431, L95
 McCarthy, P. J., Heckman, T., & Van Breugel, W. 1987, *AJ*, 93, 264
 Melnick, J., & Terlevich, R. 1988, in *Proc. 2d Workshop, High Energy Astrophysics*, ed. G. Borner (Berlin: Springer), 155
 Nomoto, K., Kumagai, S., & Shigeyama, T. 1991, in *AIP Conf. Proc. 232, Gamma-Ray Line Astrophysics*, ed. N. Prantzos & P. Durouchoux (New York: AIP), 236
 Nomoto, K., Shigeyama, T., Kumagai, S., & Hashimoto, M. 1988, *Proc. Astron. Soc. Australia*, 7, 490
 Nomoto, K., Thielemann, F. K., & Yokoi, K. 1984, *ApJ*, 286, 644
 Ohashi, T., et al. 1990, *ApJ*, 365, 180
 Pinto, P. A., & Woosley, S. E. 1988, *Nature*, 333, 534
 Rephaeli, Y., Gruber, D., Persic, M., & MacDonald, D. 1991, *ApJ*, 380, L59
 Rieke, G. H., et al. 1980, *ApJ*, 238, 24
 Rothschild, R. E., Mushotzky, R. F., Baity, W. A., Gruber, D. E., Matteson, J. L., & Peterson, L. E. 1983, *ApJ*, 269, 423
 Schaaf, R., Pietsch, W., Biermann, P. L., Kronberg, P. P., & Schmutzler, T. 1989, *ApJ*, 336, 722
 Seaquist, E. R., & Odegard, N. 1991, *ApJ*, 369, 320
 Skibo, J. G., & Ramaty, R. 1992, *A&AS*, 97, No. 1, 145
 Soifer, B. T., Sanders, D. B., Madore, B. F., Neugebauer, G., Danielson, G. E., Elias, J. H., Lonsdale, C. J., & Rice, W. L. 1987, *ApJ*, 320, 238
 Sreekumar, P., et al. 1994, *ApJ*, 426, 105
 The, L.-S., Burrows, A., & Bussard, R. W. 1990, *ApJ*, 352, 731
 The, L.-S., Clayton, D. D., & Burrows, A. 1991, in *IAU Symp. 143, Wolf-Rayet Stars and Interrelations with Other Massive Stars in Galaxies*, ed. K. A. van der Hucht & B. Hidayat (Dordrecht: Kluwer), 537
 Ulvestad, J. S., & Antonucci, R. R. J. 1994, *ApJ*, 424, L29
 Völk, H. J., Klein, U., & Wiełbinski, R. 1989, *A&A*, 213, L12
 Watson, M. G., Stanger, V., & Griffiths, R. E. 1984, *ApJ*, 286, 144
 Woosley, S. E., Pinto, P. A., & Hartmann, D. 1989, *ApJ*, 346, 395
 Woosley, S. E., & Weaver, T. A. 1986, in *Radiation Hydrodynamics in Stars and Compact Objects*, ed. D. Mihalas & K.-H. A. Winkler (New York: Springer), 91